

Chapter 4

Quasi Mutually Coupled Active Impedance Source Converter

4.1 Introduction

Peng introduced the concept of the Z source inverter in 2003 [53]. The Z source inverter utilises the zero state of the inverter configuration for boosting. Therefore, the shoot through pulses are given to the inverter during zero state which facilitate the charging of inductor. Alternatively, if EMI causes false turn ON of both the inverter switches in the same leg, then, instead of severe fault, current through Z source inverter switches is restricted by the series inductor. Therefore, Z source inverter is immune to EMI problems. In VSI, dead time is required to avoid the shoot through fault, however, Z source converter inherently provides shoot through fault protection. Single stage conversion, absence of DC link capacitance and high boosting capability are the other key benefits of Z source inverter [114]. The Z source inverter was tested for the drive application that confirmed its capability under various operating conditions [56]. Although, the converter has merits but it draws discontinuous input current and its operation is restricted by the range of $m + d < 1$. This imposes the limitation on the boosting ability of the converter. This means the higher the duty cycle, lower will be the modulation index and vice-versa. From the output THD point of view, inverter operation in lower modulation index is not recommended. So to achieve smooth output, the modulation index need to be kept at relatively higher value. This again reduces the boosting ability.

Inrush current issue is resolved by placing the impedance network after the inverter

[61] and discontinuous input current is eliminated by the introduction of quasi Z source converter [59]. But these converters do not address the limitation of gain. Diode assisted and capacitor assisted network for enhancing the gain of the converters are proposed in literature [81]. The switched inductor network arrangement was also integrated with Z source and quasi Z source configuration for increasing the gain [75]. This network further generalized in [77] for VSI and CSI based applications. In 2016, enhanced Z source converter is proposed to achieve higher boosting which uses the switched Z-impedance network [83]. These networks use increased number of passive element for enhancing the gain. In [66], switched boost inverter is proposed to reduce the number of passive element at the cost of a switch. To improve the gain of SBI, it is reconfigured and termed as current fed SBI.

With the advancement in the gain, recent trend is now shifted to the coupled inductor network. A higher boosting is attainable by the use of coupled network with reduced number of passive element. In [115], [91], a magnetically coupled network is developed for higher boosting which uses one coupled inductor and one capacitor. Trans qZSI is improved version in terms of continuous input current [90]. In line of magnetically coupled inductor various network like Improved Trans-qZSI [62], LCCT-ZSI [116], T-qZSI [87], T-ZSI [117], Asymmetrical T-ZSI [118] and Y-source [94] are proposed. A comparison between few Z source converters is presented in table-4.1.

Table 4.1: Merits and demerits of Z source converters

Impedance Network Topology	Merits	Demerits
Z source	<ul style="list-style-type: none"> • Elementary topology for ZSI 	<ul style="list-style-type: none"> • Discontinuous input current • High voltage stress across capacitor
Quasi Z source	<ul style="list-style-type: none"> • Reduced stress across passive component • Continuous input current 	<ul style="list-style-type: none"> • Limited gain
Enhanced Z source	<ul style="list-style-type: none"> • Higher voltage gain than ZSI/qZSI 	<ul style="list-style-type: none"> • Higher component count
Switched inductor	<ul style="list-style-type: none"> • Higher voltage boost than ZSI/qZSI • Lower voltage stress than ZSI/qZSI 	<ul style="list-style-type: none"> • Large passive component
T/trans Z source	<ul style="list-style-type: none"> • Higher voltage gain than ZSI/qZSI • Reduced component count than ZSI/qZSI 	<ul style="list-style-type: none"> • Still limited gain
TZ source	<ul style="list-style-type: none"> • Better Gain than previous ZSI 	<ul style="list-style-type: none"> • Two coupled inductor
LCCT	<ul style="list-style-type: none"> • Continuous input current 	<ul style="list-style-type: none"> • Gain is limited with $n=1$
Diode assisted/ Capacitor assisted	<ul style="list-style-type: none"> • Higher voltage boost than ZSI/qZSI • Lower voltage stress than ZSI/qZSI 	<ul style="list-style-type: none"> • Large passive component count
Y source	<ul style="list-style-type: none"> • Higher voltage gain • Better utilization of input voltage 	<ul style="list-style-type: none"> • Limited gain • Three winding inductor design is difficult.

Recently, A- source impedance network is proposed [119]. Unlike other converters which incorporate two winding transformer, this integrates the concept of mutual coupling based on auto transformer principle. This arrangement makes the effective turns ratio of

2) Input current is continuous without any chopping phenomenon so reduced input filter is required when connected to solar or battery system.

3) Highest gain in this category of the converter as on date.

4.3 Operation and steady state analysis of the converter

For operation and steady state analysis, the converter parameters are assumed to be ideal. The diode and switch voltage drop is equal to zero, while the three phase inverter is modelled as constant current source. The mutually coupled inductor is assumed to be sufficiently tight so that leakage inductance is zero. So it can be thought that the voltage and number of turns relation holds tightly i.e. ($V_{L2} = \frac{n_2}{n_1}V_{L1}$).

Operation

The operation of the QMCAIS is divided into three parts namely shoot through state, active State and zero state. Dark lines are showing the current flow path while faded line indicates no current flow.

Shoot through state: Shoot through state is governed by charging of the inductor. During this state the inductor charges through the short circuit path provided by inserting shoot through pulses in the inverter operation. Charging is initiated by providing shoot through pulses which turn on both the switches of the same leg (like S_1 & S_4) and switch S as shown in Fig-4.2. If the duty cycle is defined as d then the time period for which shoot through pulses are given is dT_s .

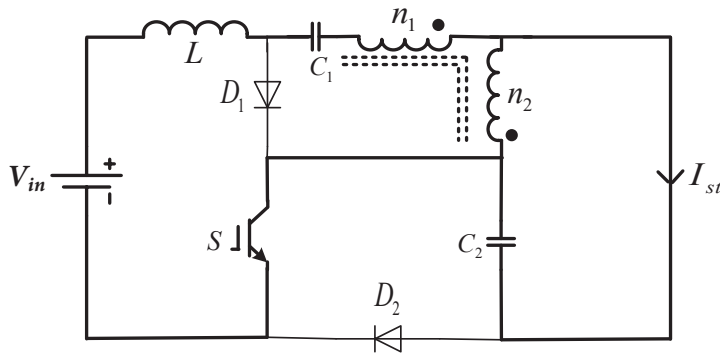


Figure 4.2: Shoot through state

Active state: This state is similar to the inverter operation for supplying the power to the load. The inverter is operated in its usual form. The energy stored during the shoot through interval now freewheels through the load. In the active impedance network, diode D_1 and D_2 comes into conduction and switch S remains OFF. The current flow path is indicated in Fig-4.3.

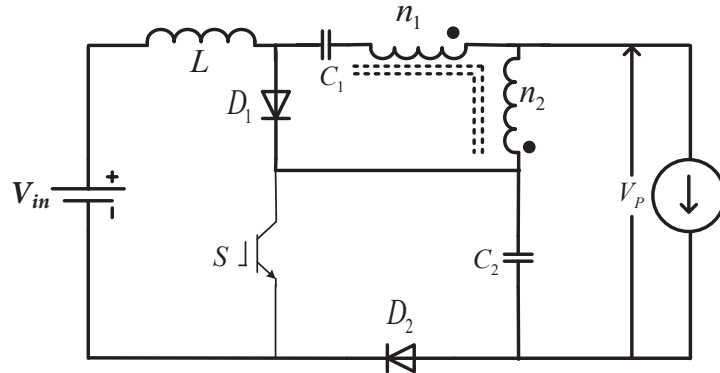


Figure 4.3: Active state

Zero state: This state is also known as load freewheel period. In this state, the load is disconnected from the supply and freewheel through the diode connected in parallel across the inverter switches. Diode D_1 and D_2 still remains ON while switch S is in OFF position. The equivalent circuit showing the current flow is indicated in Fig-4.4.

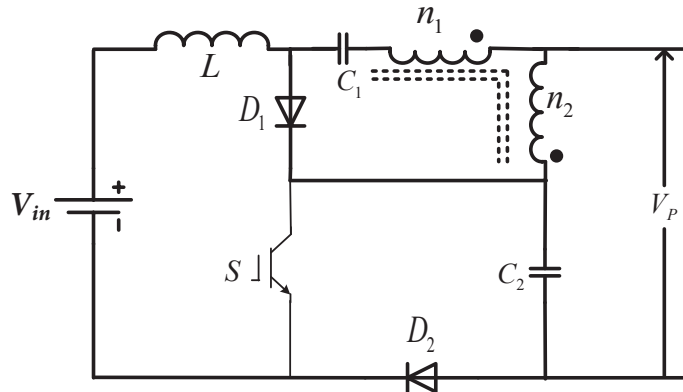


Figure 4.4: Zero state

Steady state analysis

During steady state analysis, the inductor current is assumed to be ripple free.

Shoot through interval: The switch S is ON and diodes D_1 and D_2 are reverse biased. Applying KVL in the circuit shown above, the voltage across input inductor is given as

$$V_{in} - V_L + V_{C1} + V_{L1} + V_{L2} = 0 \quad (4.1)$$

Voltage V_{L1} in terms of V_{L2} is given by

$$V_{L1} = \frac{n_1}{n_2} V_{L2} \quad (4.2)$$

Voltage V_{L2} in terms of capacitor voltage V_{C2} is

$$V_{L2} = V_{C2} \quad (4.3)$$

Combining Equ-(4.1), Equ-(4.2), and Equ-(4.3) , the inductor voltage is

$$V_L = V_{in} + V_{C1} + V_{C2} \left(1 + \frac{n_1}{n_2} \right) \quad (4.4)$$

Non-shoot through interval: In this period the diode D_1 and D_2 are in forward bias condition while switch S is off. Similar to earlier case, using KVL in circuit indicated in Fig-4.3, the voltage across input inductor is given as

$$V_L = V_{in} - V_{C2} \quad (4.5)$$

The voltage across inductor can also be written as

$$V_{in} - V_L + V_{C1} + V_{L1} - V_P = 0 \quad (4.6)$$

Equ-(4.5) and Equ-(4.6) results into

$$V_{L2} = -\frac{V_{C2}}{\left(1 + \frac{n_1}{n_2} \right)} \quad (4.7)$$

By applying the energy balance theory, the equation across inductor L_2 is given by

$$\int_0^{dT_s} V_{L2} dt + \int_{dT_s}^{T_s} V_{L2} dt = 0 \quad (4.8)$$

Combining Equ-(4.3), Equ-(4.7) and Equ-(4.8) yield

$$V_{C1} dT_s - \frac{V_{C2}}{\left(1 + \frac{n_1}{n_2} \right)} (1 - d) T_s = 0 \quad (4.9)$$

By rearranging, V_{C1} in terms of V_{C2} is written as

$$\frac{V_{C1}}{V_{C2}} = \frac{1-d}{dK} \quad (4.10)$$

where

$$K = 1 + \frac{n_1}{n_2}$$

Similarly, by applying energy balance theory across input inductor, the equation is written as

$$\int_0^{dT_s} V_L dt + \int_{dT_s}^{T_s} V_L dt = 0 \quad (4.11)$$

Combining Equ-(4.4), Equ-(4.5) and Equ-(4.11)

$$\left(V_{in} + V_{C1} + V_{C2} \left(1 + \frac{n_1}{n_2} \right) \right) d + (V_{in} - V_{C2}) (1 - d) = 0 \quad (4.12)$$

The capacitor voltage V_{C1} is

$$V_{C1} = \frac{dK}{1 + d^2 - d(2 + K)} V_{in} \quad (4.13)$$

and capacitor voltage V_{C2} is

$$V_{C2} = \frac{1-d}{1 + d^2 - d(2 + K)} V_{in} \quad (4.14)$$

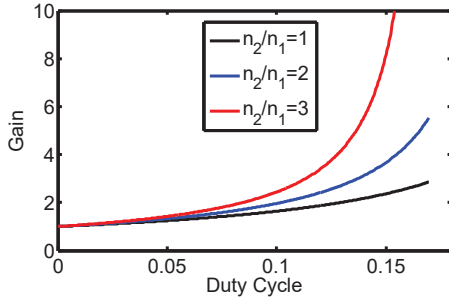


Figure 4.5: Gain vs duty cycle

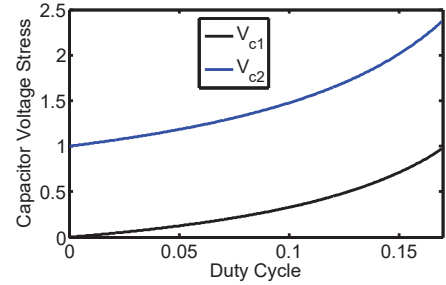


Figure 4.6: Capacitor voltage stress

For output voltage calculation, non shoot through state is taken into consideration (during shoot through it is zero). The output voltage is written as

$$V_P = V_{C2} - V_{L2} \quad (4.15)$$

Putting the value V_{L2} from non shoot through interval and substituting V_{C2} results

$$V_P = \frac{1}{1 + d^2 - d(2 + K)} V_{in} \quad (4.16)$$

This is the voltage available at the DC link across the inverter having capacitor at its terminal. For three phase inverter, the output AC peak voltage per phase in terms of DC link voltage is written as

$$V_{ac} = \frac{m \cdot V_P}{2} \quad (4.17)$$

where m is modulation index of the inverter. Constant boost control is applied for the operation of QMCAIS. The gain of the proposed converter against duty cycle at different number of turns ratio is plotted in Fig-4.5. The voltage stress across the capacitor is also plotted against duty cycle at unity turns ratio in Fig-4.6.

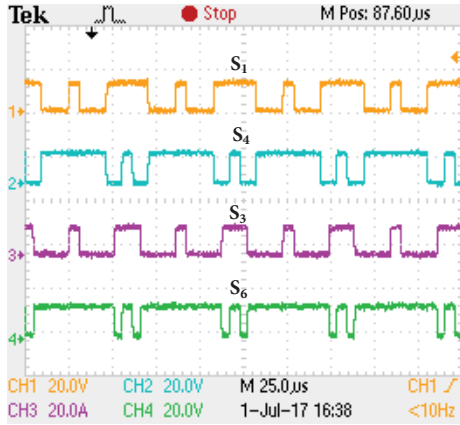


Figure 4.7: Control pulses for S_1 , S_4 , S_3 , S_6

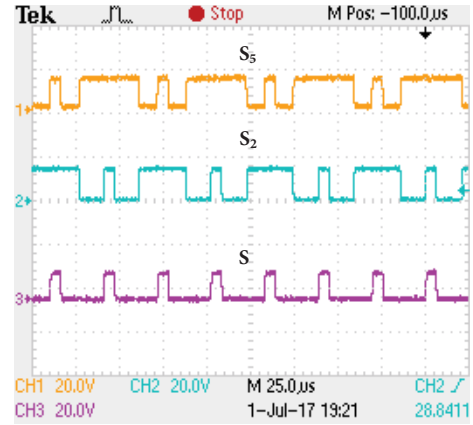


Figure 4.8: Control pulses for S_5 , S_2 , S

4.4 Experimental study

The proposed converter is validated through experimental analysis. The parameters for the experimental analysis are taken as follows: $V_{in}=25$ V, $R_{ac}=50$ Ω , $L=1$ mH, $f_s=50$ kHz, $m=0.75$, $d=0.19$, $L_f=1$ mH, $C_f=1$ μ F. The QMCIAS is tested with simple boost control technique, however to maximize the gain of the converter other techniques can be used. The control pulses for simple boost technique for the different switches are shown in Fig-4.7 and Fig-4.8. Due to leakage effect of coupled inductor, output DC link boosted voltage for the converter at given operating point is around 84 V which is less by 5 V

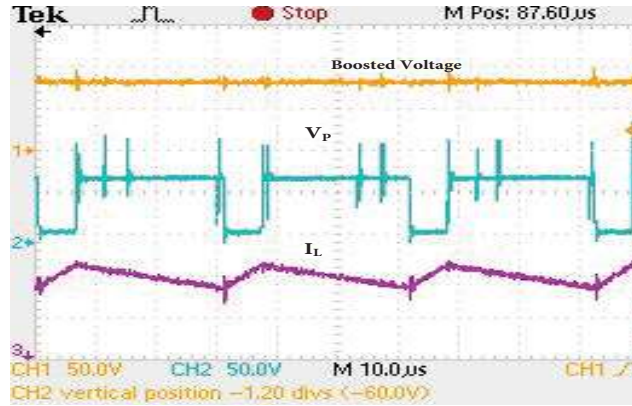


Figure 4.9: a) Boosted voltage b) DC link voltage c) Input inductor current [Ch1 : 50V/div, Ch2 : 50V/div, Ch3 : 2A/div]

as compared to theoretical value. The DC link voltage V_P is zero during shoot through period while it is equal to boosted voltage in active state. The input inductor current (I_L) is continuous in nature, which ensures continuous current mode. The coupled inductor currents i_{L1} and i_{L2} are shown in Fig-4.10. For the coupled inductor, the part which is in series with the capacitor C_1 observes negative inductor current during NST while other part has positive current. At $m=0.75$ modulation index, the output AC voltage per phase is 31 V as shown in Fig-4.11. Therefore, it can be concluded that even at AC terminal higher boosting is achieved.

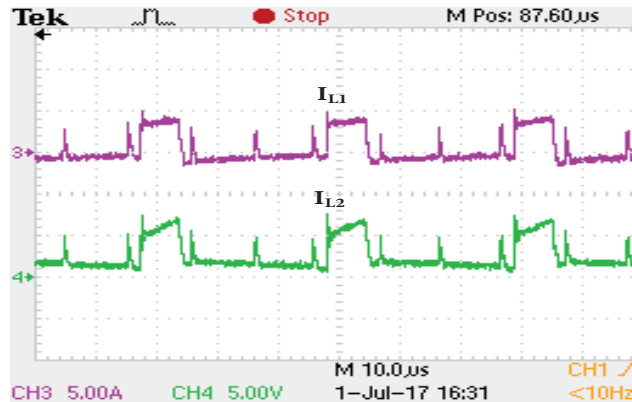


Figure 4.10: Coupled inductor currents [Ch3 : 5A/div, Ch4 : 5A/div]

The current in input inductor is shown in Fig-4.9(iii) which is continuous in nature. This makes the proposed converter a potential candidate in distributed renewable applications.

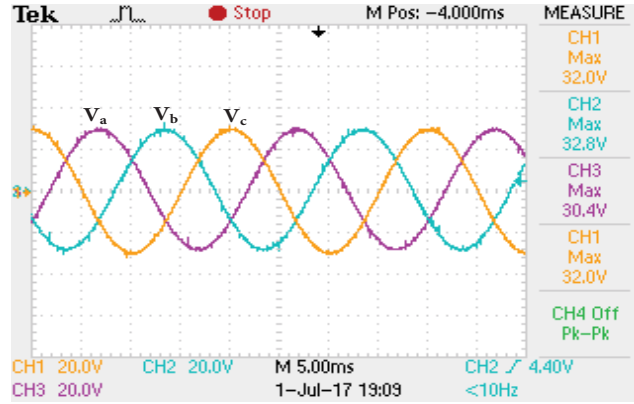


Figure 4.11: Three phase ac voltage [$Ch1 : 20V/div, Ch2 : 20V/div, Ch3 : 20V/div$]

4.4.1 Dynamic response analysis

For dynamic analysis of the proposed converter, four cases are considered. In all the cases, the converter is subjected to different operating conditions.

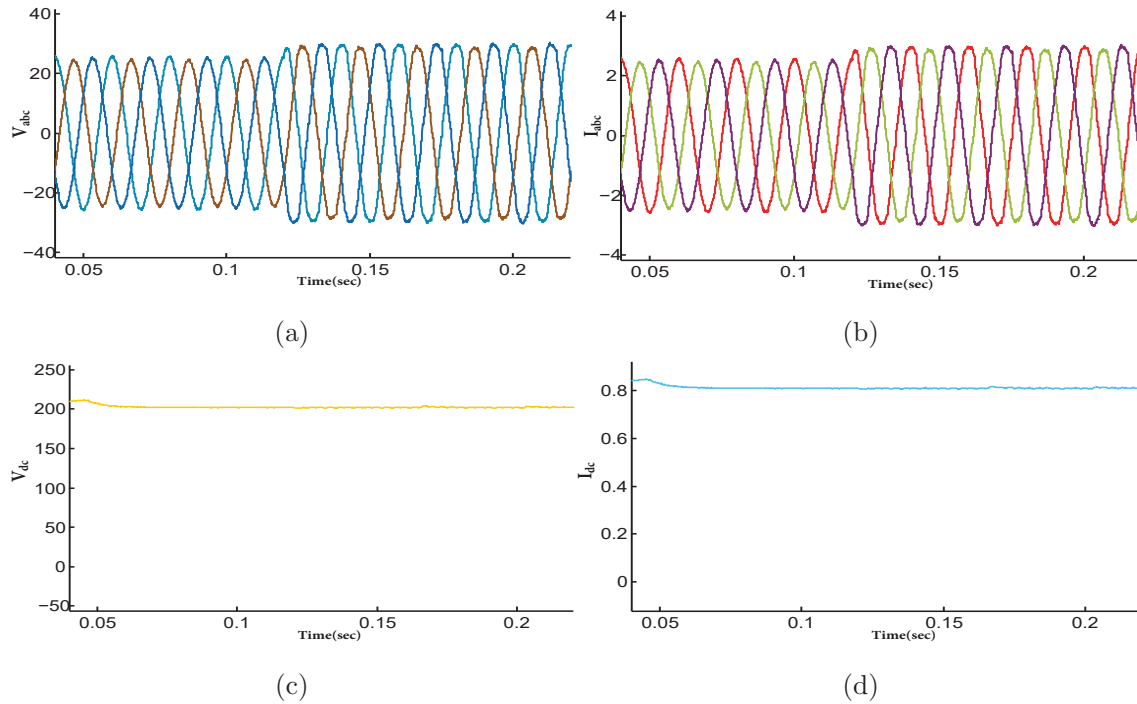


Figure 4.12: Behaviour under AC voltage tracking

Behaviour under AC voltage change

To demonstrate the behaviour under AC voltage change, the step change in AC voltage is initiated at $t=0.12$ sec. The AC voltage is increased from 25 V to 30 V as shown in

Fig-4.12a quickly. Corresponding to this, AC current is also changed as shown in Fig-4.12b. However, the DC voltage and DC load current is constant as shown in Fig-4.12c and Fig-4.12d, respectively. This confirms that the controller is able to operate independently.

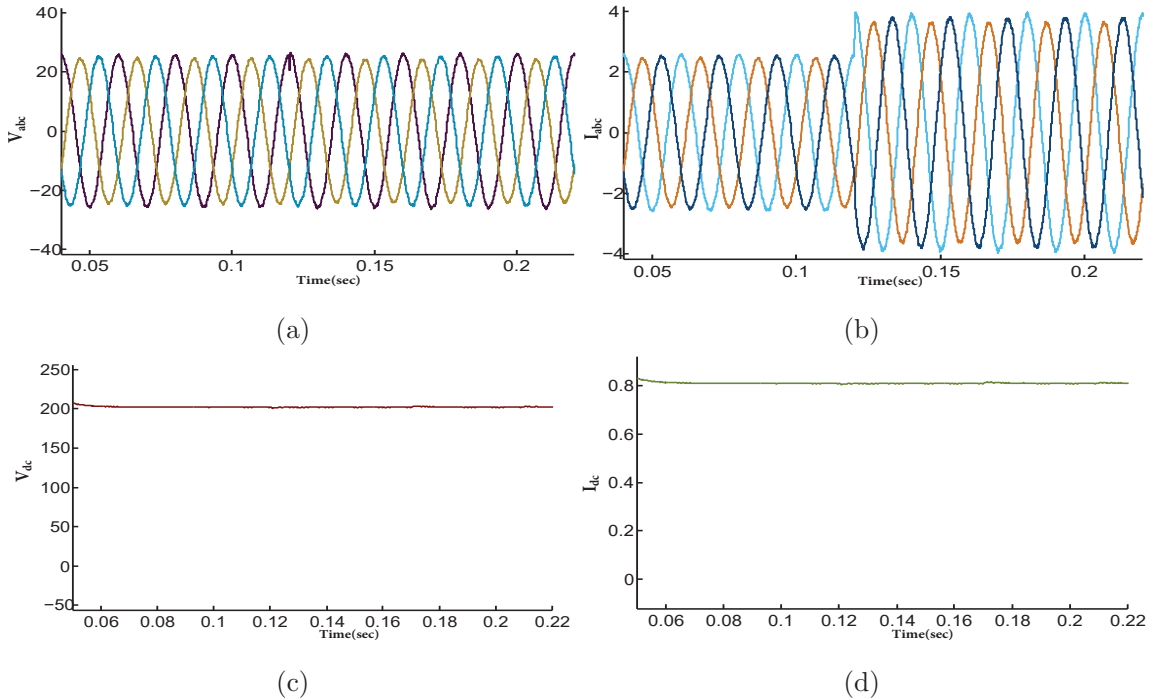


Figure 4.13: Behaviour under AC load change

Behaviour under AC load change

For evaluating performance under change in AC load, a 33% step change in AC load is applied at $t=0.12$ sec. The AC load current is increased from 2.5 A to 3.7 A as shown in Fig-4.13b while AC voltage is constant as shown in Fig-4.13a. Moreover, the DC voltage and DC current are constant as shown in Fig-4.13c and Fig-4.13d respectively. These conditions ensure that the proposed converter is able to operate independently in AC load change.

Behaviour under DC voltage tracking

To validate the robustness of DC voltage controller under reference voltage tracking, a change in reference input voltage is provided at $t = 0.12$ s. The DC voltage is changed from 200 V to 250 V instantly, as shown in Fig-4.14c. The DC controller is able to

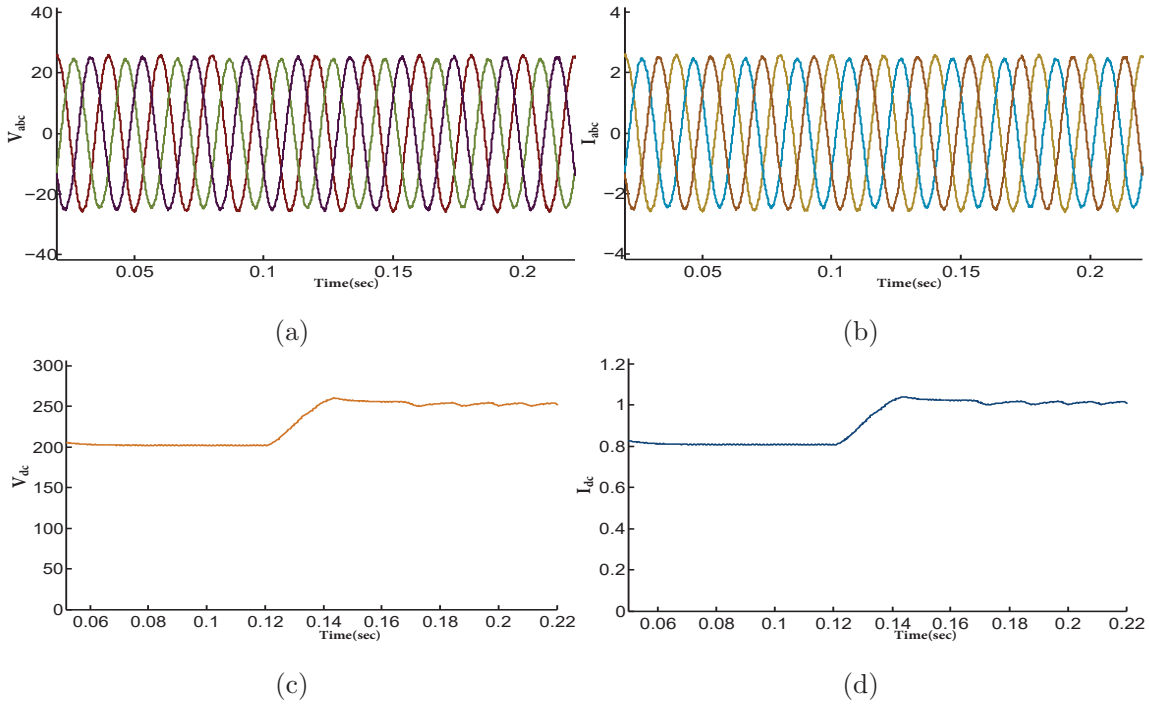


Figure 4.14: Behaviour under DC voltage tracking

maintain reference voltage after 0.02s which indicates that controller response to change in DC load voltage is bit sluggish. This sluggishness is due to higher order of system. The AC voltage controller is not affected by DC changes as shown in Fig-4.14a and Fig-4.14b which ensures independent control.

Behaviour under DC load change

In this case, the controllers ability under DC load change is evaluated. A step increase in load is applied at $t = 0.12s$. Due to this, a sharp increase in load current from 0.8 A to 1.13 A is observed as shown in Fig-4.15d. After an initial dip in voltage, DC voltage stabilizes to its steady state value as shown in Fig-4.15c. After load change, the ripple in DC voltage becomes higher due to higher DC load. Furthermore, change in DC load does not affect the AC voltage and current as shown in Fig-4.15a and Fig-4.15b.

4.5 Conclusion

A mutually coupled inductor based impedance source converter is proposed in this chapter. This converter is able to provide its maximum gain in the range of duty cycle $0 < d < 1/4$.

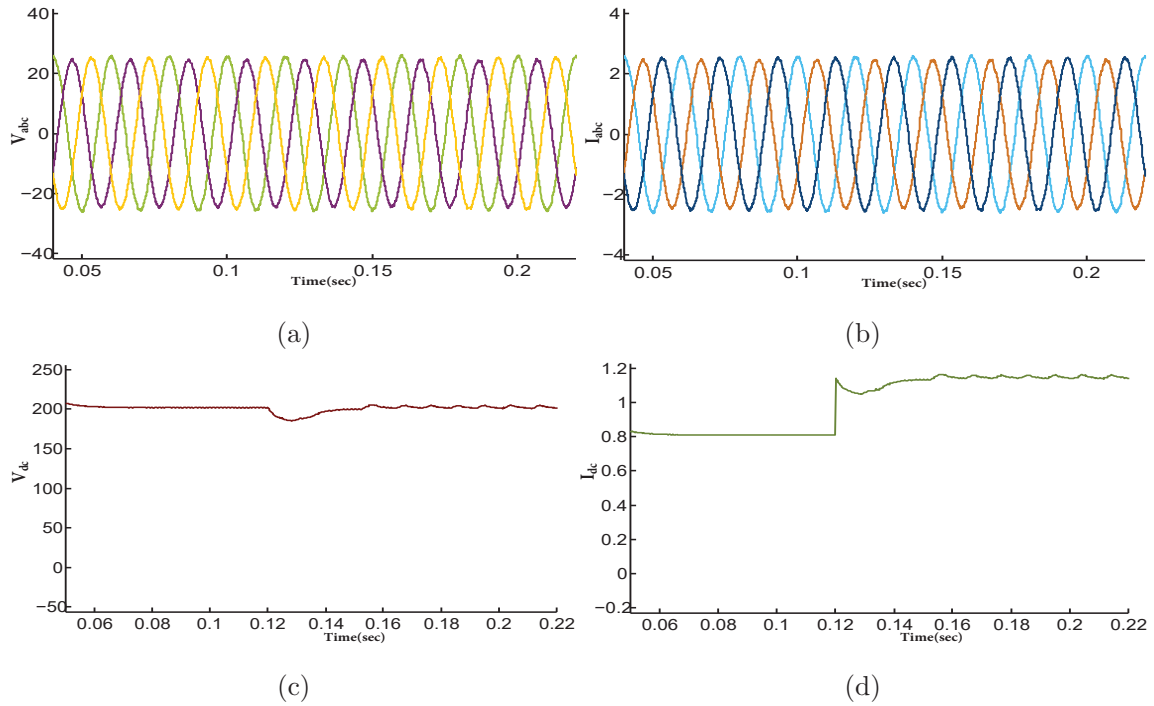


Figure 4.15: Behaviour under DC load change

This means to achieve the same gain as the conventional boost converter the proposed converter reduces the stress across the switches and capacitors present in the circuit. Moreover, the current is continuous in nature that would reduce filter requirement at the input stage. The converter is validated experimentally and achieved AC voltage at $d=0.19$ is 31 V which is higher than the input 25 V. Moreover, the dynamic response of the proposed converter is demonstrated for four different cases. In all the cases, the performance of the converter is satisfactory.

Although the gain of the proposed coupled inductor is high, however, due to two level inverter, it has higher THD. In the next chapter, a Z-source based multilevel will be proposed. The proposed multilevel converter have features such as high gain, lower THD, reduced EMI and dead time issues.